An Analogy to Bi-Elliptic Transfers Incorporating High and Low-Thrust

Steven Owens[*] and Malcolm Macdonald.[†]
University of Strathclyde, Glasgow, G1 1XJ, Scotland, E.U.

Nomenclature

g – standard gravitational acceleration, m/s^2

μ - gravitational constant, km^3/s^2

m_{dry} – spacecraft mass without fuel, kg

m_{wet} – spacecraft mass with total fuel, kg

m_{highF} – high-thrust system fuel mass, kg

m_{HSTF} – hybrid system fuel mass, kg

m_{02} – spacecraft mass after phase 1 of the transfer, kg

ΔV_{high} – high-thrust only system ΔV, m/s

ΔV_H – high-thrust portion of hybrid system ΔV, m/s

ΔV_L – low-thrust portion of hybrid system ΔV, m/s

I_{spH} – high-thrust system specific impulse, s

I_{spL} – low-thrust system specific impulse, s

I_{sp}^{HH} – Hohmann Vs HST critical specific impulse ratio

I_{sp}^{BH} – bi-elliptic Vs HST critical specific impulse ratio

T – low-thrust system thrust value, N

r_i – initial orbit radius, km

r_t – target orbit radius, km

r_c – circular transfer orbit, km

[*] PhD Candidate, Advanced Space Concepts Laboratory, steven.owens@strath.ac.uk.
[†] Associate Director, Advanced Space Concepts Laboratory, malcolm.macdonald.102@strath.ac.uk, Associate Fellow of the AIAA.

a_1 – semi-major axis between r_i and r_c, km

R1 – target/initial orbit ratio

R2 – circular/initial orbit ratio

*R2** – critical circular/initial orbit ratio

t_1 – hybrid transfer phase 1 duration (high-thrust), s

t_2 – hybrid transfer phase 2 duration (low-thrust), s

t_T – total hybrid transfer duration, s

I. Introduction

THIS note introduces an orbit transfer enabled through the use of high and low thrust propulsion technologies. To date, research in the area of high and low-thrust hybrid propulsion transfers has focused on the use of such systems for sequential orbit raising maneuvers, where the high-thrust system delivers the spacecraft to an intermediate orbit between the initial and final orbit [1–3] and the low-thrust system then completes the orbit raising maneuver. The orbit transfer introduced here, named a Hohmann-Spiral Transfer (HST), is fundamentally different to this and analogous to the high-thrust bi-elliptic transfer [4]. The HST initially uses two high-thrust impulses, firstly to reach an apoapsis beyond the target via an elliptical orbit and then secondly to circularize at this apoapsis radius. Hence, rather than following an elliptical trajectory towards the target circular orbit from the apoapsis, as in a bi-elliptic transfer, the low-thrust propulsion system propels the spacecraft along a spiral trajectory to the final orbit.

A generalized form of the critical specific impulse ratio that takes into consideration both the high and low specific impulse systems to determine the point at which an HST consumes the same amount of fuel as either a Hohmann or bi-elliptic transfer is derived. Additionally, the scenario where the transfer starts in an elliptical orbit, with apoapsis at an altitude coinciding with the target circular orbit is considered, such a scenario is equivalent to a Geostationary Transfer Orbit; the circular and elliptical initial condition cases are shown in Fig. 1. The generalized form is subsequently applied to these different scenarios. The following assumptions are applied throughout this analysis; orbits are co-planar, finite burn losses are ignored and only the gravitational force of the Earth is considered.

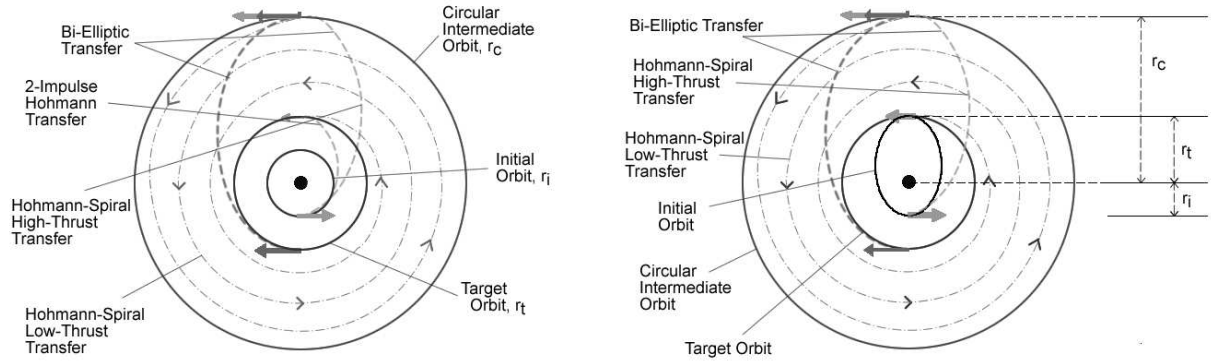

a b

Fig. 1 Orbit Definition (a – Circular Starting Orbit, b – Elliptical Starting Orbit)

II. Critical Specific Impulse Derivation

The critical ratio for the Hohmann and HST is referred to as I_{sp}^{HH} and for the bi-elliptic and HST it is I_{sp}^{BH}. They are considered separately as different orbit transfers will depend on one ratio and not the other. This means that in order to determine the most fuel efficient transfer the two ratios have to be derived independently and then compared against each other.

The high thrust and hybrid fuel mass fractions can be written as

$$\frac{m_{highF}}{m_{wet}} = 1 - exp^{\left(\frac{-\Delta V_{high}}{gI_{spH}}\right)} \tag{1}$$

$$\frac{m_{HSTF}}{m_{wet}} = 1 - exp^{\left(\frac{-\Delta V_{H}}{gI_{spH}}\right)} exp^{\left(\frac{-\Delta V_{L}}{gI_{spL}}\right)} \tag{2}$$

By equating Eqs. (1) and (2), it can be shown that the hybrid system is equivalent, or better in terms of fuel mass fraction when

$$exp^{\left(\frac{-\Delta V_{high}}{gI_{spH}}\right)} \leq exp^{\left(\frac{-\Delta V_{H}}{gI_{spH}}\right)} exp^{\left(\frac{-\Delta V_{L}}{gI_{spL}}\right)} \tag{3}$$

which can be simplified to give

$$\frac{I_{spL}}{I_{spH}} \geq \frac{\Delta V_L}{\Delta V_{high} - \Delta V_H} \tag{4}$$

confirming that a critical specific impulse ratio can be determined for the condition when the high-thrust fuel consumption is equal to the hybrid fuel consumption. Thus, for a given set of initial conditions, any specific impulse ratio above this critical value will be more fuel-efficient than the compared transfer.

A. Two-Impulse Hohmann and HST Critical Ratio

Considering Fig. 1 and Eq. (4), the following definitions give the required change in velocity, ΔV, for the low and high-thrust sections of the HST, as well as the high-thrust Hohmann transfer used for the comparison. This is true for a circular initial orbit. It should be noted that Eq. (5) is an approximate expression for the low-thrust ΔV.

$$\Delta V_L = \sqrt{\frac{\mu}{r_t}} - \sqrt{\frac{\mu}{r_c}} \quad \textit{where } r_c > r_t \textit{ (for } r_t > r_c \textit{ the equations values are switched)} \tag{5}$$

$$\Delta V_{high} = \sqrt{\frac{2\mu}{r_i} - \frac{2\mu}{r_i + r_t}} - \sqrt{\frac{\mu}{r_i}} + \sqrt{\frac{\mu}{r_t}} - \sqrt{\frac{2\mu}{r_t} - \frac{2\mu}{r_i + r_t}} \tag{6}$$

$$\Delta V_H = \sqrt{\frac{2\mu}{r_i} - \frac{2\mu}{r_i + r_c}} - \sqrt{\frac{\mu}{r_i}} + \sqrt{\frac{\mu}{r_c}} - \sqrt{\frac{2\mu}{r_c} - \frac{2\mu}{r_i + r_c}} \tag{7}$$

By then introducing the orbit ratios $R1\ \left(= \frac{r_t}{r_i}\right)$ and $R2\ \left(= \frac{r_c}{r_i}\right)$, Eq. 4 for this scenario can be simplified to give

$$\frac{I_{spL}}{I_{spH}} = {I_{sp}}^{HH} = \frac{\sqrt{\frac{1}{2R1}} - \sqrt{\frac{1}{2R2}}}{\sqrt{1 - \frac{1}{1+R1}} - \sqrt{1 - \frac{1}{1+R2}} - \sqrt{\frac{1}{R1} - \frac{1}{1+R1}} + \sqrt{\frac{1}{R2} - \frac{1}{1+R2}} + \sqrt{\frac{1}{2R1}} - \sqrt{\frac{1}{2R2}}} \tag{8}$$

Equation (4) depends on only two variables, *R1* and *R2*. In the case where the initial and target orbits are known, the critical ratio is simply dependent on the target circular orbit radius value, r_c. Varying this will give a range of transfer orbits with a given critical ratio defining the point where the hybrid system is equivalent in terms of fuel mass fraction.

From Eq. (4) it can be seen that, for the condition when the HST high-thrust ΔV equals that of the Hohmann high-thrust ΔV, a singularity exists. Beyond this singularity signifies the region in which the HST requires more fuel than the Hohmann transfer and consequently the low-thrust system would be required to add mass rather than remove it. Similarly, for the case where an elliptical starting orbit is considered, although the ΔV equations differ, it can also be shown that Eq. (4) simplifies to give Eq. (8) assuming the apoapsis coincides with the target orbit radius.

B. Three Impulse Bi-elliptic and HST Critical Ratio

Using Fig. 1, Eq. (4) and Eq. (9), which defines the ΔV_{high} for the bi-elliptic scenario, the critical specific impulse ratio comparing an HST and bi-elliptic transfer is shown in Eq. (10). The low-thrust spiral and high-thrust sections of the HST remain unchanged.

$$\Delta V_{high} = \sqrt{\frac{2\mu}{r_i} - \frac{2\mu}{r_i + r_c}} + \sqrt{\frac{2\mu}{r_c} - \frac{2\mu}{r_t + r_c}} - \sqrt{\frac{2\mu}{r_c} - \frac{2\mu}{r_i + r_c}} + \sqrt{\frac{2\mu}{r_t} - \frac{2\mu}{r_t + r_c}} - \sqrt{\frac{\mu}{r_t}} - \sqrt{\frac{\mu}{r_i}} \tag{9}$$

$$\frac{I_{spL}}{I_{spH}} = I_{sp}{}^{BH} = \frac{\sqrt{\frac{1}{2R1}} - \sqrt{\frac{1}{2R2}}}{\sqrt{\frac{1}{R1} - \frac{1}{R1+R2}} + \sqrt{\frac{1}{R2} - \frac{1}{R1+R2}} - \sqrt{\frac{1}{2R1}} - \sqrt{\frac{1}{2R2}}} \tag{10}$$

As discussed in the previous section, this equation now depends only on the variables *R1* and *R2* which are a function of the initial, target and circular intermediate orbit. If the initial and target orbits are defined the only variable undefined is *R2*. By then varying the circular intermediate orbit, a range of $I_{sp}{}^{BH}$ values can be obtained detailing the point at which the HST consumes exactly the same amount of fuel mass as the bi-elliptic transfer. As before, although the Δ*V* equations differ, Eq. (10) can be simplified and applied to an elliptical initial orbit as long as the initial apoapsis radius coincides with the target circular orbit radius.

C. Comparison of Critical Specific Impulse Ratios

Fig. 2 illustrates both Eq. (8) and Eq. (10) for a varying range of *R1* and *R2*. It can be seen from Fig. 2 that the two critical ratios intersect; as such careful consideration must be given in this region to determine which critical specific impulse ratio dominates and has control.

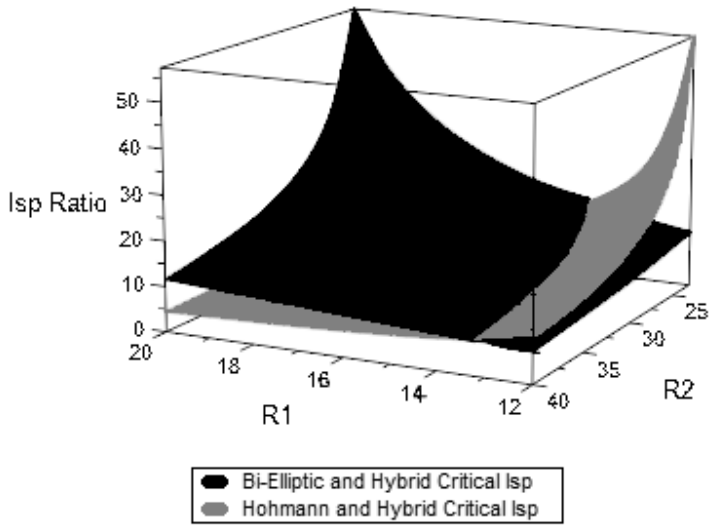

Fig. 2 Hohmann and HST and bi-elliptic and HST Critical Ratio Intersection

It is of note that a similar region of intersection, when $11.94 < R1 < 15.58$, was found by Escobal when comparing the Hohmann and bi-elliptic transfers [5]. Escobal found in this region it was difficult to differentiate which transfer was more fuel effective. To understand this fully, Escobal discovered that for a certain *R1* there is a critical *R2* value above which will ensure the bi-elliptic offers the most fuel-effective transfer and below which will ensure the Hohmann is the most fuel-effective transfer. Likewise, for an HST it can be determined, depending on the value of *R2*, which critical ratio must be considered to ensure the maneuver is superior. This analysis found that the range in which there was some uncertainty was the same as Escobal, i.e. $11.94 < R1 < 15.58$. The test is demonstrated, and hence provides validation for the analysis, by equating the critical ratios for each transfer type, in this case Eq. (8) and Eq. (10). It follows that

$$\sqrt{\frac{R2}{R2+1}} - \sqrt{\frac{R1}{R1+1}} + \sqrt{\frac{R1}{R2(R1+R2)}} + \sqrt{\frac{R2}{R1(R1+R2)}} + \sqrt{\frac{1}{R1(R1+1)}} - \sqrt{\frac{1}{R2(R2+1)}} - \sqrt{2}\sqrt{\frac{1}{R1}} = 0 \tag{11}$$

This can be solved for $R2_0$, corresponding to the zero of Eq. (11), within the defined range in order to identify the controlling critical equation. From the naturally decreasing form of the function, similar to Escobal, it can be said that any *R2* value greater than $R2_0$ will ensure the critical ratio, comparing a HST to bi-elliptic, has control of the system. Anything smaller will result in the critical ratio comparing HST to a Hohmann transfer assuming control. This coincides with the work of Escobal who drew a similar conclusion when determining the most efficient transfer in this region of uncertainty.

III. Time Restricted Transfers

Substituting Eq. (12), which is an extension of Newton's second law, into Eq. (2) introduces a time constraint into the analysis.

$$\Delta V_L = \frac{T}{m_{02}}(t_2) \tag{12}$$

Equation (13) and Eq. (14) introduce the time dependency for both the high and low-thrust sections of the HST while Eq. (15) allows the use of the orbit ratios previously defined. Thereafter substituting into Eq. (2) yields Eq. (16).

$$t_T = t_1 + t_2 \tag{13}$$

$$t_1 = \pi\sqrt{\frac{{a_1}^3}{\mu}} \tag{14}$$

$$a_1 = \frac{r_t}{2R1}(1 + R2) \tag{15}$$

$$\frac{m_{HSTF}}{m_{wet}} = 1 - exp\left[\left(\frac{-\Delta V_H}{gIsp_H}\right) + \left(\frac{-\left(\frac{T}{m_{02}}\left(t_T - \frac{\pi}{\sqrt{\mu}}\sqrt{\left(\frac{rt(1+R2)}{2R1}\right)^3}\right)\right)}{gIsp_L}\right)\right] \tag{16}$$

Introducing a time constraint element introduces a dependency on the thrust of the low-thrust system to ensure the transfer is completed in the restricted time. This allows a mission design space to be created.

IV. Case Study: Transfer from Geostationary Transfer Orbit to Geostationary Orbit

Table 1 provides the specification for the case-study transfer. The spacecraft data used is for the new Alphabus[‡] platform being developed to allow platforms with greater payload power and mass to accommodate the high power payload telecommunications market. Alphabus was selected as it already incorporates both high and low-thrust systems and as such offers a suitable design point to extend any analysis from. The T6 engine is a Kaufman-type ion engine with a 0.22m diameter and throttling capability over 4.5kW. It is produced by QinetiQ, Ltd. and is the latest in a series, including the T5 thruster which is present on the European Space Agency's (ESA) Gravity field and

[‡] European Space Agency. *An Extended European Capability*. 2010; Available from: http://telecom.esa.int/telecom/www/object/index.cfm?fobjectid=1139

steady-state Ocean Explorer (GOCE) satellite, produced by the company. As well as undergoing qualification for the extended range Alphabus platform, it has also been selected for the ESA BepiColombo mission to Mercury[6]. A maximum ninety day transfer duration is seen as a reasonable upper limit for a commercially viable telecommunications platform based on the experience of the authors. It is assumed that the launch vehicle places the spacecraft in Geostationary Transfer Orbit (GTO) with zero inclination to coincide with the assumption that orbits are co-planar. The mission terminates with the spacecraft in Geostationary Orbit (GEO).

Table 1 Alphabus GTO - GEO Specification

Transfer Specification	Property
Initial Orbit GTO Perigee Radius, r_i (km)	6628
Initial Orbit GTO Apogee Radius, r_t (km)	42,164
Target Orbit Radius GEO, r_t (km)	42,164
Mission Duration Limit, t_T (days)	90
European Apogee Motor Specific Impulse, I_{spH} (s)	325
T6 Thruster Specific Impulse, I_{spL} (s)	4500
Gravitational Constant, μ (m^3/s^2)	$3.986x10^{14}$
Standard Gravitational Acceleration, g (m/s^2)	9.81
Alphabus Maximum Launch (Wet) Mass , m_{wet} (kg)	8100
Calculated Parameters	
$R1(r_t/r_i)$	6.36
I_{sp}^{HH}	13.846

In order to determine the point at which the HST consumes the exact same amount of fuel as a Hohmann transfer, *R1* is calculated using the target orbit radius and initial orbit perigee radius. As shown in Table 1, *R1*=6.36 which can be used together with the critical specific impulse ratio, also in Table 1, to rearrange Eq. (8) and calculate *R2*. Upon doing this it is found that *R2* = 150.39 which represents an intermediate orbit roughly 23 times greater than GEO radius. This can then be used in association with Eq. (17) to determine the required thrust based on the information in Table 1 as,

$$T = \frac{-m_{02}\left[gI_{spL}log\left(1-\frac{m_{HSTF}}{m_{wet}}\right)+\Delta V_H\frac{I_{spL}}{I_{spH}}\right]}{t_T-\frac{\pi}{\sqrt{\mu}}\sqrt{\left(\frac{rt(1+R2)}{2R1}\right)^3}} \quad (17)$$

It is noted that in this case study m_{HSTF} has been set to equal that of a standard 2-impulse Hohmann transfer. It is found that the required thrust for this mission specification is 2193.5mN. Thus, in order to equal the fuel mass

consumption of a 2-impulse Hohmann transfer the HST requires 15 T6 thrusters rated at 150 mN, which is a standard value within the T6 operating range [7], and 11 thrusters for the maximum thrust of 210 mN demonstrated under experimental conditions[8]. To introduce a mass benefit to the system certain modifications can be made, these include, increasing the low-thrust engine specific impulse, increasing the transfer duration (which would also increase *R2*) or increasing the thrust of the system. It is understood that this technology requirement is not readily available and is unlikely to be at any point in the near future. It should be noted however, that this analysis is based on the maximum launch mass of the Alphabus platform and as the transfer duration is known to vary with the spacecraft mass it can be shown that for a realistic thrust range, as shown in Fig. 3, there is potential application for this transfer when considering spacecraft of order 1500kg. The figure highlights the spacecraft mass required at launch for a system fitting the Alphabus specification detailed in Table 1 that can deliver the satellite to GEO in the defined transfer duration of ninety days. With this initial mass and thrust range, the HST consumes the exact amount of fuel as the Hohmann transfer. For each thrust specification, the dry mass is approximately 63% of the total spacecraft mass. In the case where 3xT6 thrusters are used, the dry mass is approximately 1048kg.

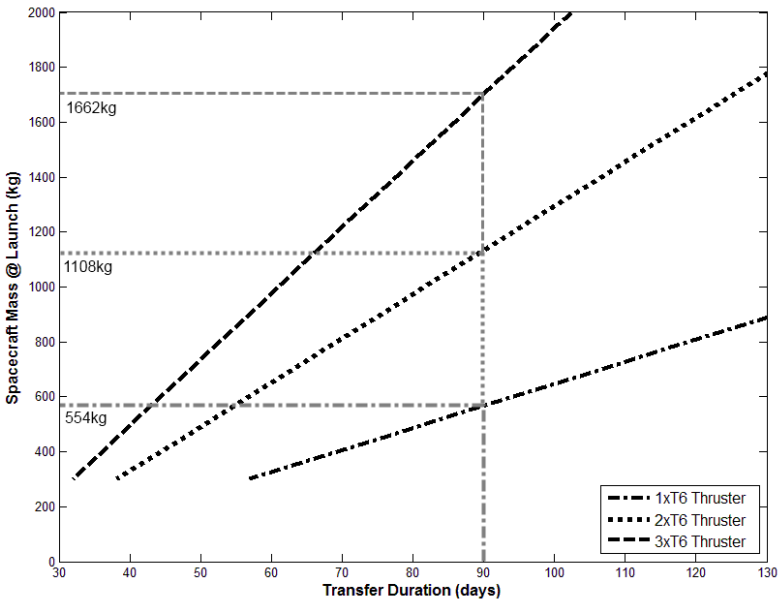

Fig. 3 Spacecraft Mass at Launch against Transfer Duration

It can be shown that if the same initial mass is used but the T6 thruster is uprated to its maximum thrust as previously defined, then a mass saving is possible. The mission duration remains unchanged but the *R2* value differs.

This is now defined at *R2*=223 which represents an intermediate orbit approximately 35 times greater than GEO radius. Table 2 shows the potential mass saving if the uprated T6 thruster is used on the spacecraft in the different configurations shown. The approximate lifetime extension is based solely on the mass saving being used by fuel for station keeping. The worst case scenario for North/South station keeping (~50m/s per year) and a desired longitude of 60° for East/West station keeping (~1.715 m/s per year) [9] are adopted. It should be noted that by reducing the lifetime extension and using the mass saving for additional payload then the platform revenue per year could be increased.

Table 2 Mass Saving with Increased Thrust

Thrust, T (mN)	Launch (Wet) Mass, m_{wet} (kg)	Dry mass, m_{dry} (kg)	Mass Saving (kg)	Approximate Lifetime Extension (Years)
1 x T6 (210)	554	357	7	11
2 x T6 (420)	1108	714	15	12
3 x T6 (630)	1662	1071	23	12

As the low-thrust system acceleration is based on the spacecraft mass after Phase 1 of the transfer it can be assumed that as the spacecraft expels mass, the acceleration will increase resulting in the spacecraft taking less than 90 days to reach the target orbit.

V. Conclusion

A novel orbit transfer method has been established that can outperform more traditional methods under certain quantifiable conditions. The point at which the Hohmann Spiral Transfer is equivalent in terms of fuel mass fraction to more conventional transfers such as the Hohmann and bi-elliptic was found by defining two critical specific impulse ratios. By varying certain parameters such as the low-thrust engine specific impulse, transfer duration or system thrust a fuel mass saving is possible with respect to either a Hohmann or bi-elliptic transfer, whichever is fuel optimal. For a spacecraft of mass less than 1700kg it was found that a Hohmann Spiral Transfer could be defined using current or near term technology and with a maximum transfer duration of ninety days consumes the same amount of fuel as a Hohmann transfer from geostationary transfer orbit to geostationary orbit. Similarly, for this same spacecraft mass region, it was found that a mass saving is possible when uprating the example thruster to its maximum output value of 210mN. The mass saving, although small (<23kg) could theoretically extend the lifetime of the spacecraft by more than 10 years assuming the mass was used solely for orbit station keeping, or be used for additional payload in order to increase the platform revenue per year.

VI. References

[1] D. Y. Oh and S. Kimbrell, "End to End Optimization of Three Dimensional Chemical-Electric Orbit Raising Missions," *28th International Electric Propulsion Conference, IEPC-03-036*. Toulouse, France, 2003.

[2] D. Y. Oh, T. Randolph, and S. Kimbrell, "End to End Optimization of Chemical-Electric Orbit Raising Missions," *Journal of Spacecraft and Rockets*, vol. 41, no. 5, pp. 831–839, 2004.

[3] D. Y. Oh and G. Santiago, "Analytic Optimization of Mixed Chemical-Electric Orbit Raising Missions," *27th International Electric Propulsion Conference, IEPC Paper 01-173*. Pasadena, California, USA, 2001.

[4] D. A. Vallado, "Fundamentals of Astrodynamics and Applications," 3rd ed., Microcosm Press and Springer, 2007, pp. 353–354.

[5] P. R. Escobal, *Methods of Astrodynamics*. John Wiley & Sons, Inc., 1968, pp. 58–67.

[6] J. S. Snyder, D. M. Goebel, R. R. Hofer, and J. E. Polk, "Performance Evaluation of the T6 Ion Engine," *46th AIAA/ASME/SAE/ASEE Joint Propulsion Conference and Exhibit*, 2010.

[7] J. Huddleson, J. Brandon-Cox, N. Wallace, and J. Palencia, "An Overview of the T6 Gridded Ion Propulsion System Pre-development Activities for Alpha-Bus," *4th Int. Spacecraft Propulsion Conference, ESA SP-555*. Cagliari, Sardinia, Italy, 2004.

[8] N. Wallace, "Testing of the Qinetiq T6 Thruster in Support of the ESA BepiColombo Mercury Mission," *4th International Spacecraft Propulsion Conference*, 2004.

[9] W. J. Larson and J. R. Wertz, *Space Mission Analysis and Design*, 2nd ed. Kluwer Academic Publishers, 1995, p. 155.